J Radioanal Nucl Chem (2015) 304:61–66
DOI 10.1007/s10967-014-3667-z

Influence of the alpha radiation on the UO_2 dissolution in high pH cementitious waters

Thierry Mennecart · Christelle Cachoir · Karel Lemmens

Received: 17 September 2014 / Published online: 5 October 2014

Abstract To assess the long-term behaviour of spent fuel in conditions of the Belgian *Supercontainer design*, dissolution tests were performed to determine the solubility and dissolution rate of depleted and Pu-doped UO_2 in synthetic cement waters. The results confirm the behaviour generally observed with UO_2 at neutral pH in absence of H_2. Due to the radiolysis of water, the produced oxidizing species oxidise the U(IV) to U(VI), inducing an increase of the uranium concentration. Consequently, the dissolution rate increases from the depleted UO_2 to the most active doped UO_2. Imposing a H_2 overpressure had no significant effect on the UO_2 behaviour.

Keywords Uranium dioxide · Dissolution rate · Alpha radiation · Hyperalkaline conditions · Cementitious water · Spent fuel

Introduction

In 2004, the supercontainer design has been selected by the Belgian Agency for Management of Radioactive Waste and Enriched Fissile Materials (NIRAS/ONDRAF) as the preferred reference design for disposal of high level waste and spent fuel [1]. This design includes the use of buffer and backfill materials based on ordinary portland cement (OPC) (Fig. 1). The Supercontainer will thus provide a highly alkaline chemical environment allowing the passivation of the overpack surface and the inhibition of its corrosion. The overpack has to prevent contact of the spent fuel with the cementitious pore water at least during the thermal phase (about 2,500 years). It will thus contribute to the containment of radionuclides, but it will also have an effect on the radionuclide release from the waste. An experimental programme has been initiated to study the stability of UO_2 as an analogue of real spent fuel in the cementitious environment of the supercontainer design, more specifically to determine the UO_2 dissolution rate, the UO_2 solubility [2, 3] and the influence of alpha radiation on the behaviour of the UO_2. This paper is dedicated to the radiation effect on the UO_2 behaviour under hyperalkaline conditions.

T. Mennecart · C. Cachoir (✉) · K. Lemmens
Waste and Disposal Research Unit, Belgian Nuclear Research Centre (SCK·CEN), Boeretang 200, 2400 Mol, Belgium
e-mail: christelle.cachoir@sckcen.be

T. Mennecart
e-mail: Thierry.mennecart@sckcen.be

Experimental

All experiments were performed at 25–30 °C under argon. Static experiments were conducted at different ratio of fuel surface area to leachant volume (SA/V of 6, 17, 130, 257 m^{-1}) with and without iron or iron/magnetite as redox buffer in order to determine the UO_2 solubility. No duplicate experiments were done. Dynamic tests were run at three different flow rates (20, 12, 8 μL min^{-1}) to determine the UO_2 dissolution rate.

Static and dynamic experiments were performed with depleted and with ^{238}Pu-doped UO_2 powders to simulate the spent fuel activity as function of time (Table 1). The various doped materials were manufactured by ITU [4] using ^{233}U (0.3 %) to serve as corrosion indicator and ^{238}Pu to generate the alpha dose. They represent the alpha-activity of spent fuel with an average burnup (45–55 GWd tHM^{-1}) respectively 150, 2,000, 11,000 and 89,000 years after discharge from the reactor. Depleted UO_2 was used as surrogate for a very old spent fuel (>10^9 years).

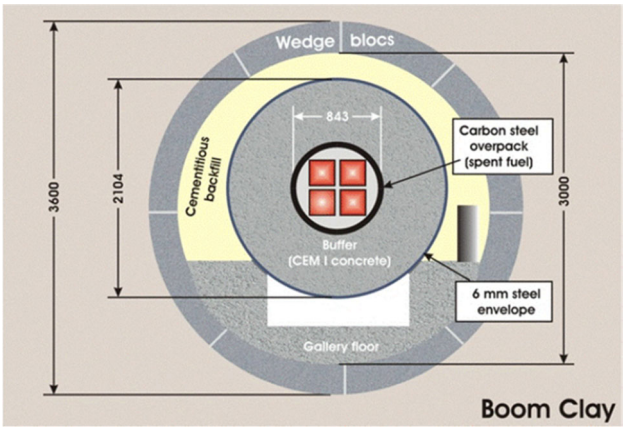

Fig. 1 Supercontainer design

The leachants were synthetic cement waters. Their composition was based on the expected chemical evolution of the concrete after contact with Boom Clay water, which has been estimated by geochemical calculations, assuming equilibrium between the pore water and mineral phases in the cement [6]. The pH (at 25 °C) in the concrete buffer is expected to decrease from 13.5 (Young Cement Water) to 12.5 (Evolved Cement Water) and further to pH ~ 12 (Old Cement Water). Later on, the pH will decrease below 12. Table 2 gives the composition of the three cementitious waters for which the most important parameters are the pH, the concentration of calcium, sodium and potassium, which may interact strongly with uranium [7–9].

Additional static tests were also carried out at pH 13.5 (YCW) with F2 Pu-doped UO_2 with H_2 overpressure of 0.5 bar or of 5 bar to determine if H_2 may reduce the uranium release as reported in literature [5].

Before the start of the experiments, the materials were previously annealed to remove the U(VI) traces (Argon/5 % H_2 gas at 1,000 °C).

All details concerning the Pu-doped fuels, the cement water composition, and the setup parameters were previously described in [3].

The released ^{238}U for depleted UO_2 and ^{233}U for Pu-doped UO_2 was measured by ICP-MS and alpha-spectrometry respectively. The dissolution rate was calculated based on the not filtered concentrations [NF], to make sure that all released U is considered, and normalized to the exposed surface area of the materials. This surface area was estimated based on literature survey [10] considering the geometrical surface of the UO_2 powder, calculated with the average grain size of the fraction, and afterwards corrected with the surface roughness factor of three [11]. The resulting values are given in Table 1. The soluble concentration was determined based on the ultrafiltered (UF) samples using 30,000 MWCO filters (< 2.6 nm). The speciation of the uranium (U(IV)/U(VI)) was determined for the soluble/UF fractions by anion-exchange chromatography in HCl medium [12]. All speciations and all filtrations were carried out in an argon glove box ($pO_2 < 1$ vppm, $pCO_2 < 0.1$ vppm) to limit oxidation of the samples.

Results and discussion

For the tests with depleted UO_2, the ^{238}U concentrations are shown. For the tests with α-doped UO_2, the normalized

Table 1 Description of tested UO_2 batches

Fuel type	α-Activity (MBq g^{-1} UO_2)	Fuel age (~years)	^{233}U weight fraction[a]	^{238}Pu weight fraction[b]	Surface area[c] ($\times 10^{-2}$ m^2 g^{-1})
F1	240	150	3.9×10^{-3}	4.0×10^{-4}	1.4
F2	36	2,000	4.2×10^{-3}	5.5×10^{-5}	3.2
F4	17	11,000	4.2×10^{-3}	2.5×10^{-5}	3.2
Depleted UO_2	0.01	$>10^5$			3.2

[a] Mass of ^{233}U/mass of doped UO_2

[b] Mass of ^{238}Pu/mass of doped UO_2

[c] Based on literature survey [10] and calculated with the average grain size of the powder fraction

Table 2 Composition of the cement waters (YCW, ECW and OCW) in mol L^{-1}

	Na	K	Ca	Al	Si	SO_4^{2-}	CO_3^{2-}	pH
YCW	1.4×10^{-1}	3.3×10^{-1}	6.5×10^{-4}	$<7 \times 10^{-6}$	2.0×10^{-4}	2×10^{-3}	9.3×10^{-4}	13.5
ECW	1.6×10^{-2}	2.2×10^{-4}	1.3×10^{-2}	1.1×10^{-5}	1.8×10^{-4}	3×10^{-6}	4.8×10^{-4}	12.5
OCW	3.7×10^{-3}		7.3×10^{-4}	3.7×10^{-6}	1.5×10^{-4}	4×10^{-5}	1.4×10^{-4}	11.7

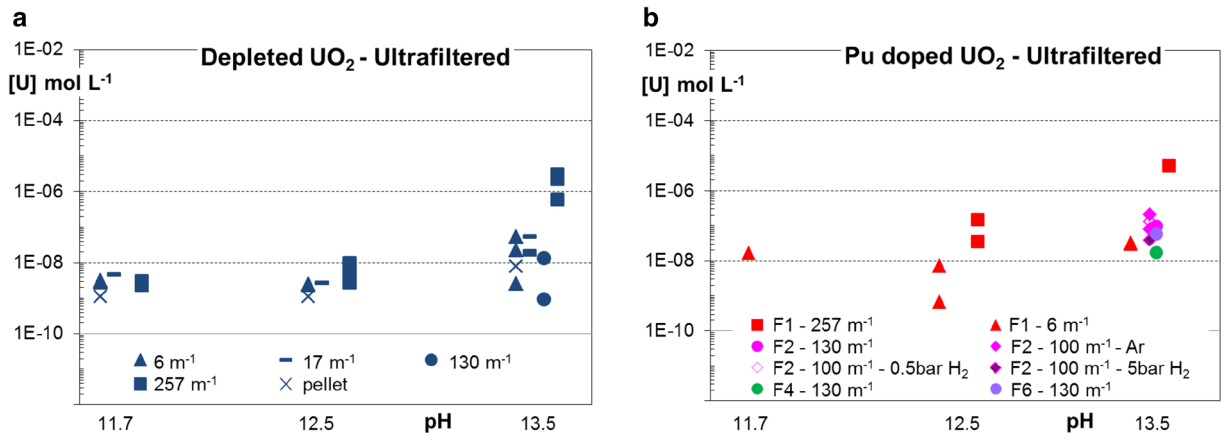

Fig. 2 Soluble uranium concentration (UF) in mol L^{-1} as function of pH. **a** Without α-radiation, **b** with α-radiation. To avoid overlapping of the data points, data for different SA/V are shown next to each other per type of cement water (no variation of the pH). Experimental uncertainties have been calculated by error propagation ($2\sigma = 15$ %), and are included in the size of the symbols. The presence of redox buffer caused the variation observed for samples with identical SA/V and identical pH

^{233}U concentrations are indicated, i.e. the measured molar ^{233}U concentration, divided by the ^{233}U mole fraction in the UO_2. In a previous paper the influence of the ratio SA/V, the pH, the water composition and the influence of calcium was discussed [2]. In this paper, we focus on the influence of the alpha radiation on the solubility and dissolution rate of UO_2.

Influence of the alpha radiation on the UO_2 concentration

The soluble uranium concentration is plotted in function of the pH for tests with depleted UO_2 (Fig. 2a) and for Pu-doped UO_2 (Fig. 2b).

In absence of alpha-radiation, the soluble uranium concentration ranged between 10^{-9} and 10^{-8} mol L^{-1} for pH 11.7 and for pH 12.5, and 10^{-9} to 2×10^{-6} mol L^{-1} for pH 13.5 (Fig. 2a), the highest concentrations corresponding to tests at high SA/V for all pH. Uranium speciation showed that the measured soluble U(IV) concentration for these tests was close to the U(IV) solubility of 3×10^{-9} mol L^{-1}, and independent of pH as reported in [13]. While the U(IV) was constant, the U(VI) concentration slightly increases when pH increases due to the increasing complexation of U(VI) with OH^- [2, 14]. As little radiolytical oxidation is expected with depleted UO_2, the U(VI) in the system was attributed to (pre)-oxidation by traces of oxygen in the glove box. This explained why increasing the surface area exposed to the leachant, increases also the soluble U(VI) concentration.

In presence of alpha-radiation (Fig. 2b), the soluble uranium concentration slightly increased to the range of 10^{-8}–10^{-7} mol L^{-1} for pH 11.7 and for pH 12.5, and of 10^{-8}–10^{-5} mol L^{-1} for pH 13.5. Although this trend is weak, the increase is significant considering the small experimental uncertainty on the measured uranium concentrations. We assume that the higher uranium concentration is due to radiolysis, and therefore is mainly U(VI). Indeed, the soluble uranium concentration was higher (except for one data point) than the U(IV) solubility of about 3×10^{-9} mol L^{-1} at pH 7–14 [13].

The results raise questions about the possible interaction between the high pH and the radiolytical UO_2 oxidation. There is no evidence in literature for increased radiolysis at high pH. Our results seem to confirm this. As the total U concentrations (not filtered) did not depend on the pH [2], it is likely that the high pH better removed the oxidized U(VI) by complexation with OH^-, leading to higher soluble concentrations, without accelerating the radiolytical oxidation. Nevertheless, it cannot be excluded that the formation of a thick oxidized (Ca containing) UO_{2+x} layer, protecting the UO_2 layer underneath, would finally cause a decrease of the radiolytical UO_2 oxidation. This may explain why the dissolution rate of spent fuel seems to be lower in the Ca rich ECW than in other media [15].

The presence of hydrogen is also an important factor susceptible to affect the behaviour of the spent fuel. Indeed, hydrogen (from radiolysis or anaerobic steel corrosion) is known to counteract the oxidative dissolution of fresh spent fuel at neutral pH [5]. At high pH, the measured soluble uranium concentration was close to 10^{-7} mol L^{-1} under 0.5 bar H_2 overpressure, slightly decreasing towards 5×10^{-8} mol L^{-1} under 5 bar H_2 overpressure. However, these concentrations were equivalent to the soluble uranium concentrations determined under Ar atmosphere in similar experimental conditions (Fig. 2b), so the H_2 gas had little or no effect. This result appears contradictory to the soluble uranium concentration of 10^{-9} mol L^{-1}

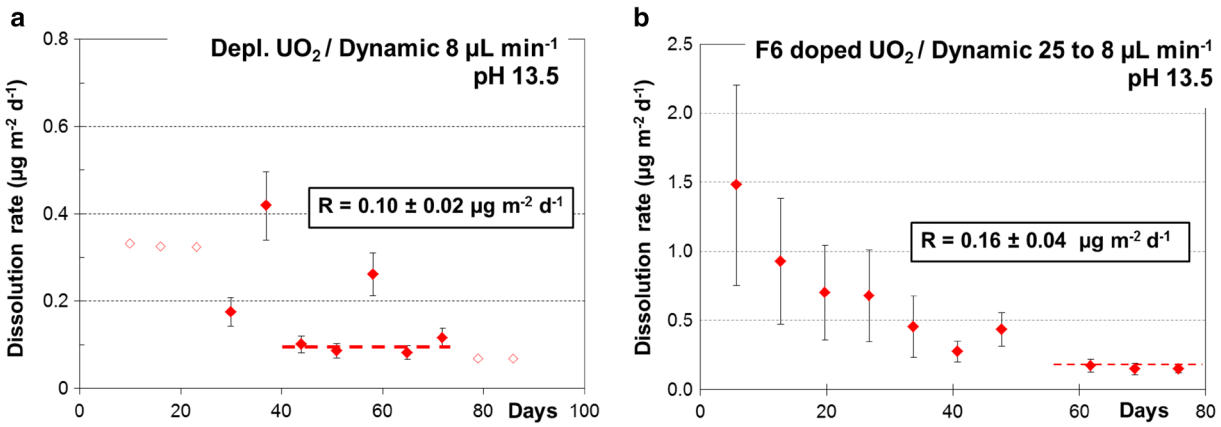

Fig. 3 Dissolution rate in function of the duration time of the dynamic experiments with **a** depleted UO_2 and **b** Pu-doped UO_2 (F6) in contact with the YCW at pH 13.5. The *open symbols* correspond to [U] below detection limit

reported for tests performed with a cladded segment of spent fuel at pH 12.5 under 3.5 bar H_2 overpressure in the same cementitious water [15]. The difference may be explained by the fact that spent fuel contains metalloids (the so called ε-particles) that are known to play the role of catalyst for uranium reduction, whereas the Pu doped UO_2 does not contain these particles.

As the soluble concentrations stopped increasing with time in most of the static tests with or without hydrogen and with an without alpha-radiation, this suggests that uranium in solution may have reached equilibrium with U(VI) phases likely to form in these conditions. The solubility range of these phases would be 10^{-8}–10^{-5} mol L^{-1}, depending on pH, [Ca] and [Si] [2, 7–9, 14]. Although the measured uranium concentrations are compatible 1—with the solubility of $CaUO_4$ and $Ca_2U_2O_7$ [2, 7, 8, 14], and 2—with geochemical calculations done with Geochemist workbench coupled to Moldata [16] as thermodynamic database, macroscopic observations of such phases are still lacking.

Influence of the alpha radiation on the dissolution rate

The evolution of total uranium concentration (not filtered) was used to estimate the UO_2 matrix dissolution rate of depleted UO_2 and Pu-doped UO_2.

We distinguish dissolution rates from dynamic and static experiments. Dynamic experiments are more suitable to study the direct effect of pH or dose on the UO_2 dissolution rate because they suffer less from experimental artefacts e.g. pre-oxidation of the surface, secondary phase formation, colloid formation. Saturation of the solution with uranium would yield dissolution rates proportional to the flow rate, and could thus mask the effect of the alpha-radiation. Therefore, the tests are performed at flow rates selected such that the outcoming solution is undersaturated with regard to the UO_{2+x} surface, and where the dissolution rate thus depends less on the flow rate. Figures 3, 4, 5, 6 show the evolution of the dissolution rate in function of the time for the experiments with alpha doped UO_2 (F6, F4, F2 and F1) and depleted UO_2 in contact with the YCW (pH 13.5). For depleted UO_2 and F6 Pu-doped UO_2, the uranium concentration mainly decreased with time before reaching a plateau (Fig. 3). The initial high concentrations are due to the release of U(VI) produced by the oxidation by traces of atmospheric oxygen in the glove box. The final uranium concentration was about 10^{-9} mol L^{-1}, close to U(IV) solubility [13] and consequently may be ascribed to non-oxidative dissolution. The rate is represented by a dashed line in Fig. 3. The resulting dissolution rates are 0.1 and 0.16 µg m^{-2} d^{-1} for depleted UO_2 (0.01 MBq $g^{-1}UO_2$) and F6-doped UO_2 (1.4 MBq $g^{-1}UO_2$), respectively, for flow rate of 8 µL min^{-1}. These results support the hypothesis that depleted UO_2 can surrogate 'old spent fuel' (F6).

For F2, F4, and F1 Pu-doped UO_2, the uranium concentrations were in the range of 10^{-8}–10^{-7} mol L^{-1}. They are higher than for depleted UO_2 and F6 Pu-doped UO_2 because of radiolysis, and thus more representative for U(VI). Although these concentrations may approach the saturation of certain U(VI)-phases the dissolution rate appears independent of the flow rate (Figs. 4, 5, 6a). The dissolution rate was thus averaged for all data whatever the flow rate, and represented by the dashed lines in Figs. 4, 5, 6a. For F2 doped UO_2, two dynamic tests were performed. In the first test, two separate steady state levels (rates) were obtained (Fig. 5a). The lowest rate (1.9 µg m^{-2} d^{-1}) was obtained with data from mostly ultrafiltered samples. The higher rate (6.9 µg m^{-2} d^{-1}) was measured only for not-filtered samples and probably gives a better estimation of the dissolution rate. For this reason, the lower rate is considered as less reliable. These variations may be due

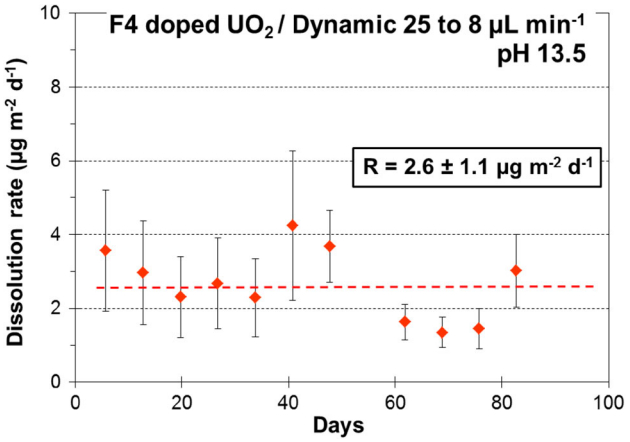

Fig. 4 Dissolution rate in function of the duration time for the dynamic experiments with Pu-doped UO_2 (F4) in contact with the YCW at pH 13.5

also to changes in the solution during the period of time between the sampling and the analyses. This experiment was therefore repeated (Fig. 5b), giving a range of dissolution for F2 doped UO_2 of 6.9–28.6 µg m^{-2} d^{-1}. The resulting dissolution rates are 2.6 µg m^{-2} d^{-1}, 6.9–28.6 µg m^{-2} d^{-1}, and 12.1 for F4 (17 MBq $g^{-1}UO_2$), F2 (36 MBq $g^{-1}UO_2$) and F1 (245 MBq $g^{-1}UO_2$) Pu doped, respectively.

Most of the static dissolution rates may have underestimated the real matrix dissolution rate because the uranium concentration stabilized with time at levels that may correspond to a possible phase precipitation (see previous section). However in static tests with the most active Pu-doped UO_2 (F1), uranium concentration gradually increased with time up to 500 days before decreasing. The long term dissolution rate was thus determined by linear regression of the total amount of uranium dissolved per

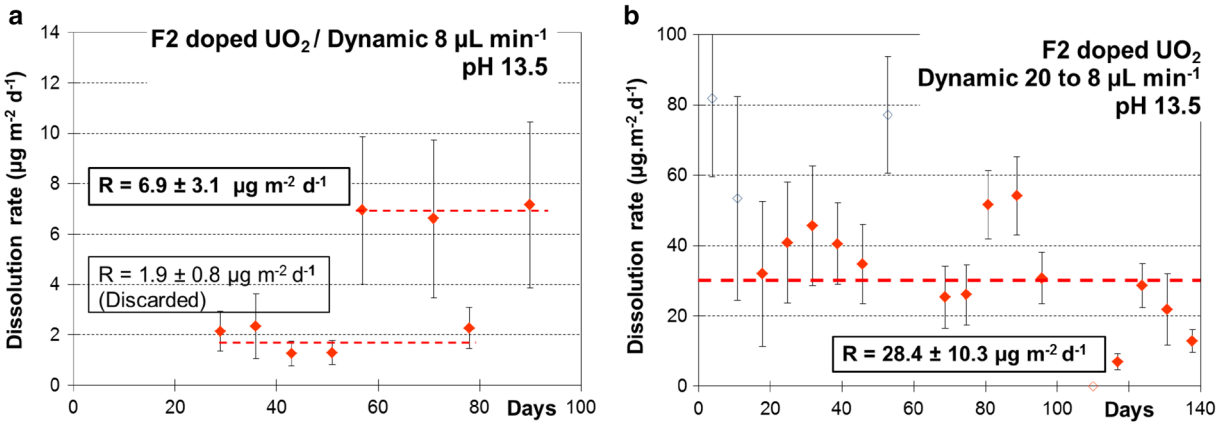

Fig. 5 Dissolution rate in function of the duration time for the dynamic experiments with Pu-doped UO_2 (F2) in contact with the YCW at pH 13.5. **a** With flow rate of 8 µL min^{-1} and **b** with varying flow rate (20–8 µL min^{-1}). The *open symbols* correspond to [U] below detection limit

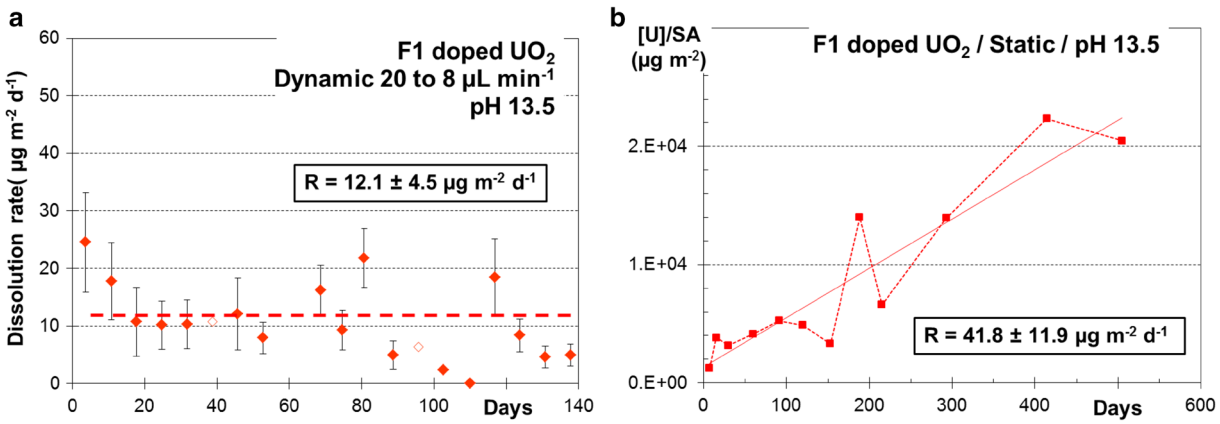

Fig. 6 Dissolution rate in function of the duration time for **a** dynamic experiments with Pu-doped UO_2 (F1) and **b** for static experiments with Pu-doped UO_2 (F1) in contact with the YCW at pH 13.5

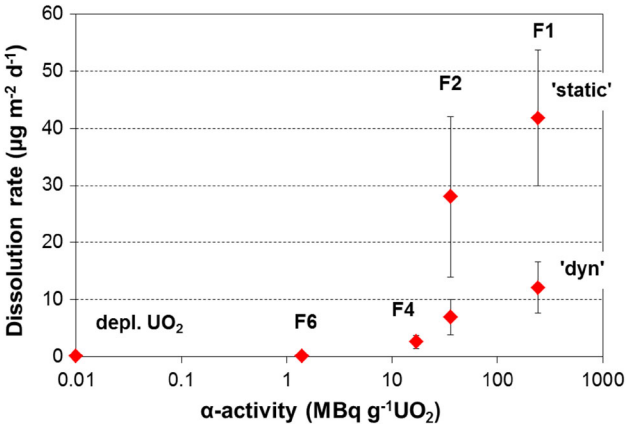

Fig. 7 Experimental dissolution rates in function of the alpha activity of the simulated UO_2 at pH 13.5

Table 3 Experimental dissolution rates at high pH compared to the rates at more neutral pH [17]

Dissolution rate (µg m^{-2} d^{-1})	Neutral pH	pH 13.5
UO_2	0.03–20	0.1–0.16
Simulated fuel without H_2	0.3–26	0.16–41

unit of surface area as a function of time (Fig. 6b). The resulting dissolution rate is 41 µg m^{-2} d^{-1}, giving a range for the dissolution rate of F1 doped UO_2 of 12.1 µg m^{-2} d^{-1} (dynamic) to 41 µg m^{-2} d^{-1} (static).

All estimated dissolution rates are plotted in function of the alpha activity of the doped UO_2 in Fig. 7. Increasing the alpha-activity of fuel clearly increases the dissolution rate from 0.1 µg m^{-2} d^{-1} for a fuel of 0.01 to 1.4 MBq $g^{-1}UO_2$ (depleted UO_2- F6 Pu doped UO_2) to 40 µg m^{-2} d^{-1} for a fuel of 250 MBq $g^{-1}UO_2$ as (F1 Pu doped UO_2). According to the data at more neutral pH in absence of H_2 gas [17], the current dissolution rates at high pH are in good agreement with the dissolution rates at more neutral pH under slightly reducing conditions (Table 3). Based on Fig. 7, we can also estimate that the alpha threshold i.e. boundary where the dissolution is controlled by the UO_2 solubility is subrogated by the oxidative dissolution of fuel, might be somewhere between 17 and 1.4 MBq $g^{-1}UO_2$.

Conclusion

The behaviour of the UO_2 matrix in alkaline cement waters was studied in static and dynamic experiments. The high pH did not increase the soluble U(IV) concentrations. As at neutral pH, the alpha radiation slightly increases the uranium release in solution due to the oxidation of U(IV) to U(VI). According to thermodynamic data, the measured U(VI) concentrations in solution are in agreement with the solubility limit of $CaUO_4$ or $Ca_2U_2O_7$. The influence of hydrogen was also investigated. No effect of hydrogen on the uranium concentration was observed with Pu-doped UO_2, because the UO_2 does not contain the catalyzing epsilon particles.

We demonstrated that the dissolution rate increases with the alpha activity of the UO_2 matrix, as reported at neutral pH. From a depleted UO_2 to a high doped level, the dissolution increases from 0.1 to 40 µg m^{-2} d^{-1}. The evolution of the dissolution rate indicates that the alpha threshold may be somewhere between 17 and 1.4 MBq $g^{-1}UO_2$ which corresponds to a spent fuel of 11,000 and 89,000 years old, respectively.

Acknowledgments This work was performed as part of the programme of the Belgian Agency for Radioactive Waste and Enriched Fissile Materials (NIRAS/ONDRAF) on the geological disposal of high-level/long-lived radioactive waste. The authors gratefully acknowledge the technical support from Ben Gielen and Regina Vercauter.

References

1. Bel JJP, Wickham SM, Gens R (2006) Mater Res Soc Symp Proc 932:23–32
2. Cachoir C, Mennecart T, Lemmens K (2014) Mater Res Symp Proc 1665, *in press*
3. Mennecart T, Cachoir C, Lemmens K (2012) Mater Res Symp Proc 1475:293–298
4. Rondinella V, Matzke Hj, Cobos J, Wiss T (1999) Mater Res Soc Symp Proc 556:447–454
5. Fors P, Carbol P, Van Winckel S, Spahui K (2009) J Nucl Mater 394:1–8
6. Wang L (2009) NIROND-TR report 2008–23
7. Moroni L (1995) Waste Manag 15(3):243–253
8. Altmaier M, Gonna X, Fanghanel T (2013) Chem Rev 113:901–943
9. Yamamura T et al (1998) Radiochim Acta 83(139–146):1998
10. Oversby VM (1999) SKB Technical report TR-99-22
11. Iglesias I, Quinones J, Rodriguez N (2008) Mater Res Soc Symp Proc 1104:NN03-07
12. Ollila K (1996) Posiva report, POSIVA-96-01
13. Neck V, Kim JI (2001) Radiochim Acta 89:1–16
14. Tits J, Fujita T, Tsukamoto M, Wieland E (2008) Mater Res Soc Symp Proc 1107:467–474
15. Loida A, Gens R, Metz V, Lemmens K, Cachoir C, Mennecart Th, Kienzler B (2012) Mater Res Symp Proc 1475:119–124
16. Wang L, Salah S, De Soete H (2014) External Report SCK-CEN-ER-257
17. Grambow B (2010) Final project report: MICADO final report